Microsyst Technol (2007) 13:1607–1613
DOI 10.1007/s00542-006-0340-7

TECHNICAL PAPER

Integration of micro-electro-mechanical deformable mirrors in doped fiber amplifiers

D. Bouyge · A. Crunteanu · D. Sabourdy · P. Blondy · V. Couderc · J. Lhermite · L. Grossard · A. Barthélemy

Received: 18 May 2006 / Accepted: 20 November 2006 / Published online: 4 January 2007

Abstract We present a simple technique to produce active Q-switching in various types of fiber amplifiers by active integration of electrostatic actuated deformable metallic micro-mirrors. The optical MEMS (MOEMS) device acts as one of the laser cavity reflectors and, at the same time, as switching/modulator element. We aim to obtain laser systems emitting short, high-power pulses and having variable repetition rate. The electro-mechanical behavior of bridge-type membranes was simulated by using electrostatic and modal 3D finite element analysis (FEA). The results of the simulations fit well with the experimental mechanical, electrical and thermal measurements of the components. In order to decrease the sensitiveness to fiber-mirror alignment we are developing novel optical devices based on stressed-metal cantilever-type geometry that allow mirror deflections up to 50 μm with increased reflectivity discrimination during actuation.

1 Introduction

For obtaining laser pulse generation in a conventional Q-switched fiber laser, a passive or active modulator (saturable absorbers, or acousto-optic, electro-optic or mechanical components) has to be introduced into the cavity (Barnes 1993). Although these conventional solutions are based on solid, mature technologies, most of them present inherent disadvantages that restrain their integration in miniature, compact laser systems: degradation of the beam quality, high insertion losses for the acousto-optic modulators (Zalvidea et al. 2005), high voltages and low modulation frequencies for the electro-optics solutions (El-Sherif and King 2003), bulkiness for mechanical choppers, low laser power levels operation for piezoelectric Bragg gratings systems (Russo et al. 2002) or lack of control of frequency and pulse width for the passive modulators. We previously reported (Crunteanu et al. 2006) on active Q-switching demonstration for an erbium-doped fiber laser (EDFA) using a deformable metallic micro-mirror like the one represented in Fig. 1. As explained there, the micro-mirror consists in a 500 nm-thick gold membrane (bridge) suspended over an actuation electrode placed 2.2 μm underneath the membrane and covered with a dielectric thin film (Al_2O_3, 200 nm thickness) for electrical isolation during actuation The laser system incorporating the optical MEMS device operates at frequencies between 20 and 120 kHz and generate short pulses (with FWHM down to 326 ns) with high peak powers, up to 100 times greater than the continuous emission (Crunteanu et al. 2006).

The MOEMS device is small, compact, highly reflective and achromatic, allowing a great integration potential. The simplicity of this pulse generation technique makes it suitable for being implemented in more complex set-ups including solid-state micro-lasers, multi-wavelength fiber lasers or different families of fiber lasers (Yb- or Er-Yb- doped) actuated independently or synchronous for wavelength mixing/tuning applications.

D. Bouyge · A. Crunteanu (✉) · D. Sabourdy · P. Blondy · V. Couderc · J. Lhermite · L. Grossard · A. Barthélemy
XLIM Research Institute, University of Limoges, 123 Av. Albert Thomas, 87060 Limoges, France
e-mail: aurelian.crunteanu@xlim.fr

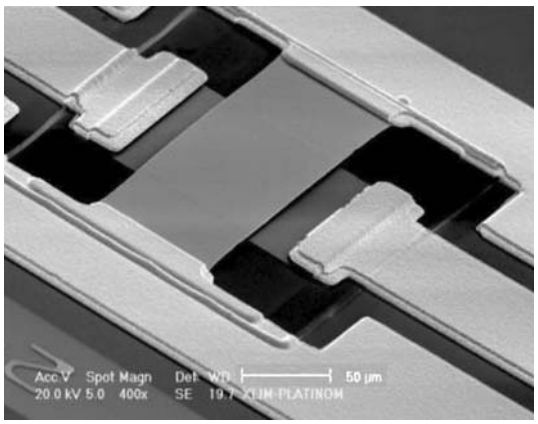

Fig. 1 Scanning electron micrograph (*SEM*) of a typical metallic micro-mirror (bar scale is 50 µm)

The images presented in Fig. 2 shows several designs based on this bridge-type membrane. Figure 2a is a matrix of 44 micro-mirrors, which can be integrated with several parallel fiber amplifiers for generation of synchronized pulse trains. The larger membrane (1×1 mm^2), which can be actuated by independent electrodes (Fig. 2b), it is planned to be used with larger, multimode laser beams for laser mode selection.

Here we report on the thermo-mechanical behaviour of the membrane mirrors through FEA simulations and experimental measurements. We present recent results of different fiber laser systems coupled with the MOEMS devices and the design and fabrication of devices with improved capabilities developed to optimise the laser Q-switch generation.

2 Bridge-type membrane

2.1 Mechanical measurement and FEM simulation

The most critical parameter for generating high-energy pulses in a Q-switched fiber laser is the modulator speed. In our case this parameter is determined, in a first-order approximation, by the mirror's mechanical primary resonant frequency (directly linked to the switching time of the mirror). In-plane tensile stresses, arising from device micro fabrication and temperature changes, may result in a significant increase of the resonant frequency and of the actuation voltage (Zhu and Espinosa 2004). In order to determine the effects of the build-in stress and operating temperature on the membrane's mechanical resonant frequency, we simulated the behavior of the membranes with different dimensions and under different temperatures, using the multi physics package of ANSYS. The experimental resonant frequency values were recorded using an electro-mechanical method presented earlier (Mercier et al. 2003). The gold-type mirrors have a relatively high mechanical resonant frequency at RT, ranging from ~65 kHz (for the 240×160 µm^2-area membranes) up to 170 kHz (for the 120×60 µm^2 ones). The material properties (considered to be isotropic in the *XYZ* directions) of the membranes are listed in Table 1. Figure 3 shows the simulation results of the mechanical resonant frequency of gold and aluminum-type membranes (0.5 µm in thickness and 80 µm in width) as a function of their lengths at room temperature (RT). We noticed that for widths values in the range of 50–160 µm, this parameter is not influencing the resonant frequency (variation of less than 3%). In the case of the gold layers the experimental measurements are very well fitted when the uniaxial tensile stress applied to the membranes has a value of 30 MPa.

Table 1 Material properties used for the simulation of metallic membrane thermo-mechanical behavior

Material property	Au	Al
Young's modulus (Gpa)	78	70
Thermal expansion coefficient (10^{-6} K^{-1})	14.2	23.5
Poisson ratio	0.42	0.345
Material density (g cm^{-3})	19.30	2.70

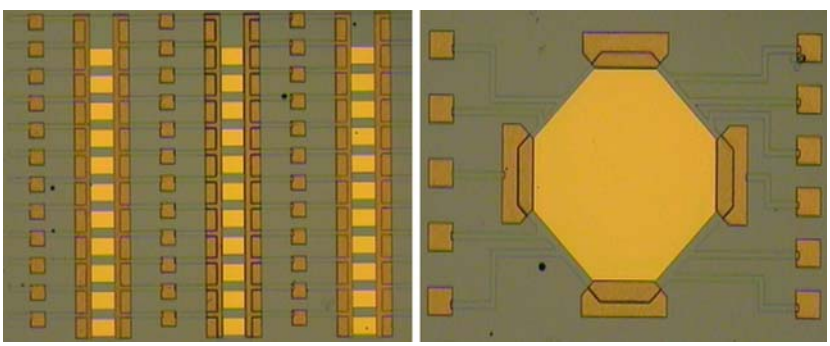

Fig. 2 Optical microscopy images of a matrix of independently or simultaneously actuated micro-mirrors (160×200 µm^2) (**a**) and of a 1×1 mm^2 large-area membrane (**b**)

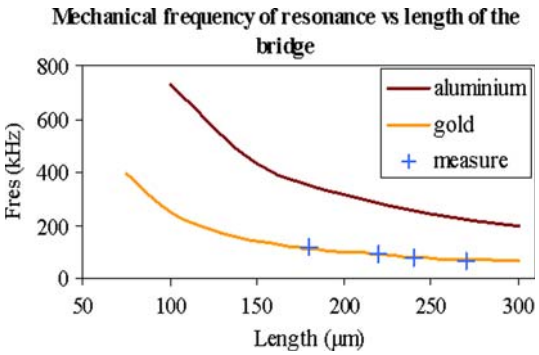

Fig. 3 Mechanical primary resonant frequency RT as a function of the membrane length (the *cross points* are for gold-type bridge experimental measurement and the *continuous lines* refer to the FEA simulations of gold-and aluminum-type bridges)

We are currently designing and implementing similar types of optical switching elements, which are intended to be faster. Lowering of the switching time of the mirrors will lead to narrower laser pulses with higher peak powers as well as higher pulse repetition rates. We produced smaller bridges with lengths ranging from 75 μm up to 150 μm, and we are currently developing aluminum-type bridges using the same fabrication process. According to the curves on Fig. 3 the mechanical resonant frequency at RT of the smaller membranes will take values between 150 and 400 kHz for the gold-type devices while for the aluminum-type ones the frequencies will be higher than 400 kHz. Figure 4 shows the temperature evolution of the resonant frequency for a 160×220 μm^2 area gold mirror undergoing a cooling-heating cycle between RT and liquid-nitrogen (LN_2) temperature (77 K). During the cooling cycle the resonant frequency is increasing up to 250 kHz but the membrane recovers its mechanical behavior when heating back to RT.

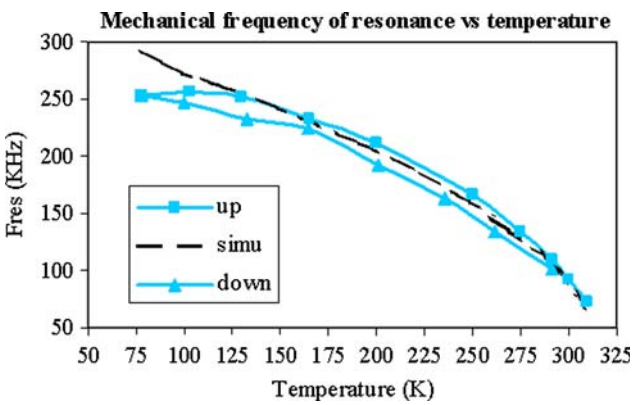

Fig. 4 Experimental measurement of F_{res} with temperature between RT and 77 K and FEA simulation (30 Mpa tensile stress) for a 160×220 μm^2 membrane

Lower temperatures increase the tensile stress of the membrane, which explain higher F_{res} values. We observed that for higher temperatures (up to 370 K) the stress turn into a compressive one that leads to buckling of the bridge and device failure.

2.2 Fiber laser systems coupled with the optical MEMS

2.2.1 Opto-mechanical characterizations of the micro-mirrors

The laser beam focused on the membranes is deflected by ~9° during switch actuation, with a good reflectivity discrimination between the on- and off- actuation states, which is enough for loss modulation of the laser cavity. Figure 5 presents the generation of laser pulses having a FWHM of 860 ns at 60 kHz actuation frequency and 700 mW mean laser power, implying pulse peak powers of ~14 W. The laser power handling of the micro-mirrors was investigated by placing them in an Er/Yb co-doped fiber laser. The amplifier was side pumped by a laser diode emitting at 915 nm with powers up to 5 W. The experiments were carried out for various levels of emitted laser power. In the non-actuated, off state, the membranes seem to sustain quite well laser powers up to 1 W (the maximum power delivered by the laser) in CW regime. In the Q-switch regime, for mean powers higher than 900 mW, the membrane degrades leading to a brutal fall of the power.

2.2.2 Dual-wavelength fiber amplifier

Because of the achromaticity of the membrane, the MOEMS element can be used with different types of

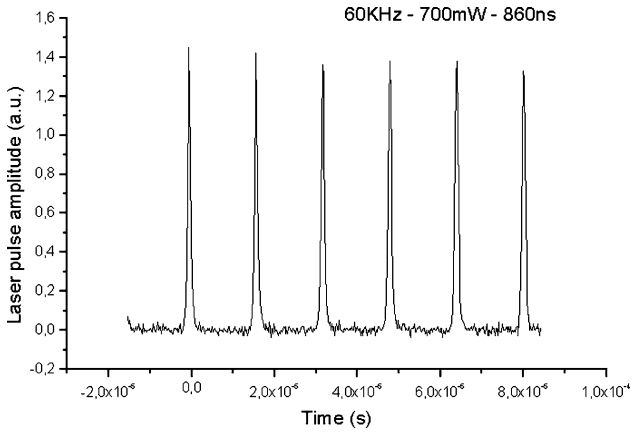

Fig. 5 Pulse train generation using an 160×220 μm^2 MOEMS at 60 kHz actuation frequency

amplifiers emitting at different wavelengths. The dual-wavelength fiber laser system depicted in Fig. 6 consists in two synchronized Q-switched fiber lasers (an EDFA and an Yb-doped fiber amplifier). Both lasers are core pumped through a wavelength division multiplexer (WDM) by a laser diode emitting up to 100 mW at 980 nm. At the ends of the two amplifiers, the two signals are mixed using a WDM (1,060/1,550 nm). The output coupler of the laser system has a 4% reflectivity (right angle cleaving of the end of the WDM fiber). The dual laser system is closed at the other end by the optical MEMS element (acting as back-end achromatic cavity mirror and Q-switch modulator).

Using the system described above we generated a perfectly superposed pulse trains coming from both lasers having FWHM of 820 ns at an actuation frequency of 30 kHz (Fig. 7). Figure 8 shows the spectral components of each pulse peaks and one can notice the well-known emissions of Yb and Er at ~1,060 nm and at ~1,550 nm, respectively. Thus, we obtained a laser system emitting synchronized pulse trains with two components in the spectral domain.

2.2.3 *Active Q-switching in an erbium-doped fiber laser (EDFA)*

In the architecture of the EDFA presented by Crunteanu et al. (2006), the back end emission of the laser is coupled to the MOEMS through an imaging system based on two confocal micro-lenses. In this way it is possible to attain pulses with peak powers of several watts and repetition rates that can be continuously tuned from 20 to 120 kHz. The duration (FWHM) of the generated pulses varies from 326 ns up to 1 µs.

Taking into account the small dimensions of the MOEMS elements, it will be very interested to realize an even more compact device, with higher integrability. A possible solution is to be freed from the imaging system. We observed that without the imaging system,

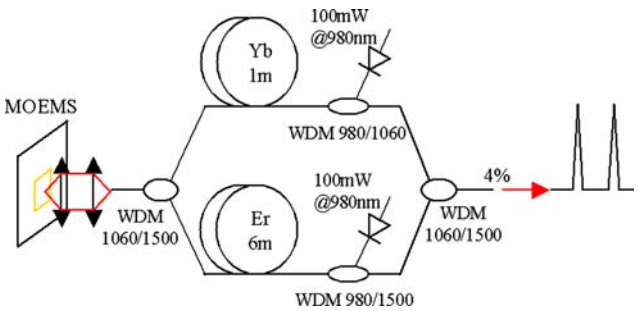

Fig. 6 Set-up of the laser fiber system emitting dual-wavelength pulses

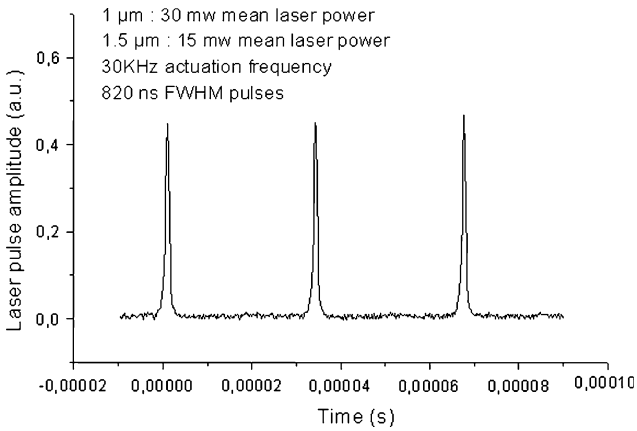

Fig. 7 Pulse train generation of the dual-wavelength fiber laser system

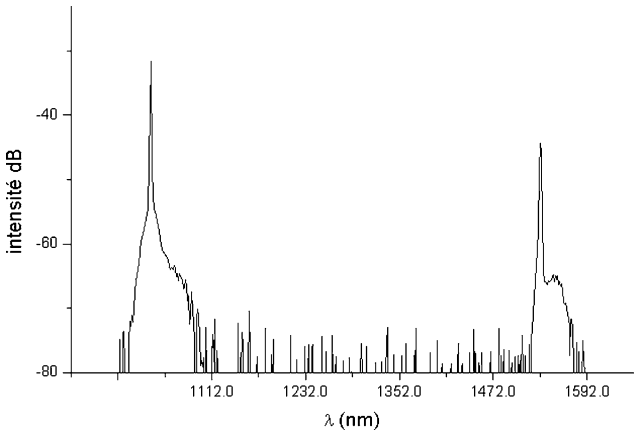

Fig. 8 Spectral emission of pulses for the Q-switched dual-laser system

the re-injection of the laser beam in the fiber amplifier is somehow reduced, resulting in a significantly decrease of the mean laser power. In spite of this reduction the beam modulation is still fast enough for the laser to pass in the Q-switching regime even when using this simple configuration. However, with the same type of micro-mirror as presented by Crunteanu et al. 2006 (80×140 µm^2 area membrane) the EDFA emits 1.4 µs FWHM pulses, at 39 kHz actuation frequency with a 7 mW mean power laser, which represents pulses with peak power of only 150 mW (Fig. 9).

3 Cantilever-type micro-mirrors

For obtaining higher reflectivity discrimination during MOEMS actuation we designed and fabricated micro-mirrors based on a cantilever-type design (Fig. 10). The design is intended to avoid the use of an additional

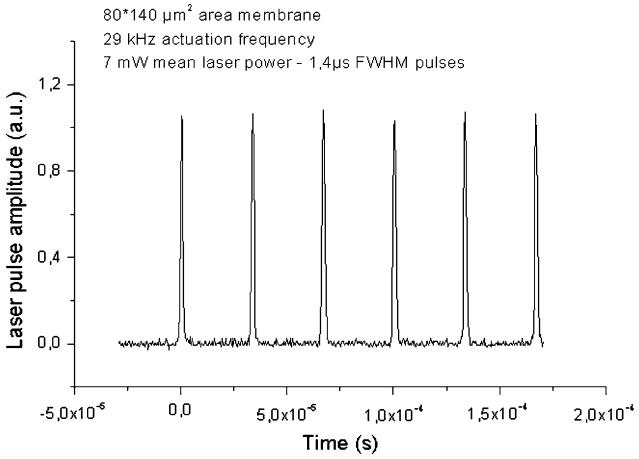

Fig. 9 Pulse train generation without the imaging system

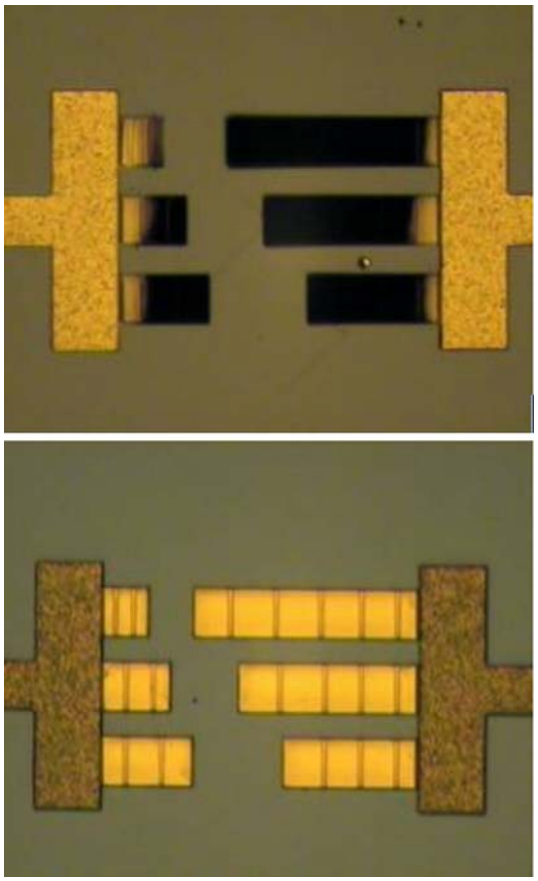

Fig. 10 Optical microscopy image of cantilever-type mirrors (100 µm widths with lengths of 100, 150, 200, 300, 400 and 500 µm, respectively) in **a** OFF-state and **b** ON-state

imaging system leading to smaller, integrated packaged system. The principle of operation of this MEMS structure has been presented by Duffy et al. (2001) and next developed by Muldavin et al. (2003). It is based on a curled metallic membrane above a conductive electrode. The stressed, up-warded, membrane is fabricated on a low resistivity Si substrate (acting as lower electrode) covered with 1 µm thermally grown SiO_2 layer (as dielectric isolator). When applying a voltage between the substrate and the cantilever, this one is attracted toward substrate due to the generated electrostatic forces.

The fabrication process for the cantilever-type mirrors starts by deposition of a two steps sacrificial layers (PMGI and S1813 photo resins) that allows to separate the metal membrane layer 0.6 µm apart from the substrate, and make 1.5 µm deep corrugations in order to provide longitudinal stiffness to the structure and successful control of the initial deformation. The membranes metallization is performed using a Cr/Au (40/800 Å) seed layer following by gold electroplating up to 1.5 µm. Next a 100 Å Cr layer is deposited in order to provide an appropriate stress gradient for the

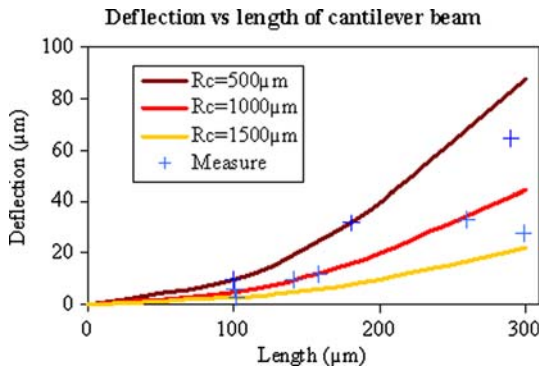

Fig. 11 Membrane deflection versus membrane length for stressed cantilever-type MOEMS (experimental measurement and analytical solution with different curvature radius of 500, 1,000 and 1,500 µm)

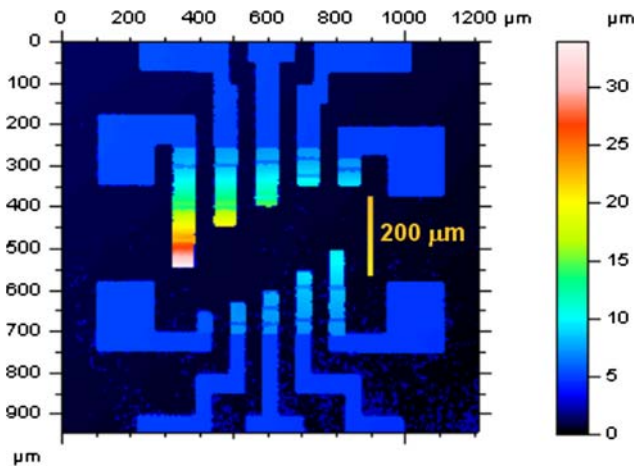

Fig. 12 Optical interferrometry top image of cantilevers-type profile

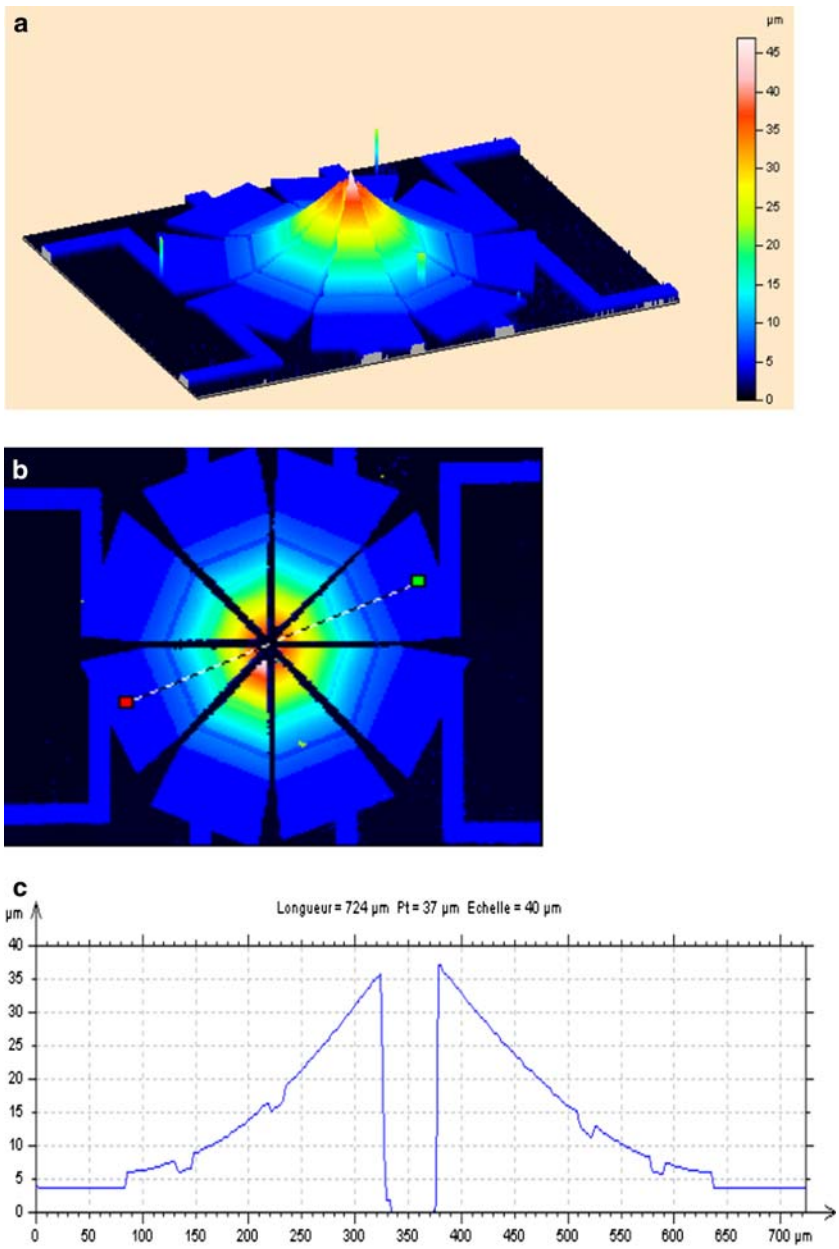

Fig. 13 3D image (**a**) top image (**b**) and profile section of triangular cantilever-type membranes obtained using optical interferometry

released membranes and the foldable areas are patterned using wet etching of the Cr/Au/Cr layers. Finally, the MOEMS components are released by wet dissolution of the sacrificial layers following by a critical point drying technique.

We fabricated cantilever-type devices with different dimensions (from 50×50 μm^2 to 300×500 μm^2) and different designs (rectangular and triangular). The simulations of the mechanical resonant frequency for the rectangular membranes gives values from ~6 kHz up to 236 kHz at RT, depending on the dimensions. The profile of the cantilevers, measured using optical interferometry shows curvature radius between 500 and 1,500 μm (Fig. 11) depending on the design and on the components dimensions (Fig. 12).

Figure 13 shows the 3D (a), the top image (b), and the profile (c) of an array of 200 μm in width and 250 μm in long triangular cantilever-type membranes. They have deflections up to 33 μm, which corresponds to a 1,000 μm radius of curvature. The incident laser beam will be deviated by ~15° after reflection on these particular micro-mirrors. The array can be used with laser beams having larger widths and may be a solution to improve the power handling capabilities of the

MOEMS. The simulated mechanical resonant frequency of this particular structure is about 45 kHz.

4 Conclusion

We developed micro-mirrors that can be integrated with various types of laser amplifiers running at different wavelengths and with different architectures. A thermo-mechanical FEM model was developed to simulate the mechanical resonant frequency of the optical elements, and the results fit well with experimental measurement. Shortening of the switching time of the mirrors will lead to narrower laser pulses with higher peak powers as well as higher pulse repletion rates. Optimization of the laser Q-switch modulation using such micro-mirrors (bridge-type and especially, cantilever-type) will enable rapid development of applications like laser wavelength mixing, laser mode selection or multi-laser emission synchronization.

References

Barnes W (1993) Q-switched fiber lasers. In: Digonnet M (eds) Rare earth doped fiber lasers and amplifiers. Marcel Dekker, New York, pp 375–391

Crunteanu A, Bouyge D, Sabourdy D, Blondy P, Couderc V, Grossard L, Pioger PH, Barthélemy A (2006) Deformable micro-electro-mechanical mirror integration in a fiber laser Q-switch system. J Opt A Pure Appl Opt (in press)

Duffy S, Bozler C, Rabe S, Knecht J, Travis L, Wyatt P, Keast C, Gouker M (2001) MEMS microswitches for reconfigurable microwave circuitry. IEEE Microw wireless components lett 11:106–108

El-Sherif AF, King TA (2003) High-energy, high-brightness Q-switched Tm^{3+}-doped fiber laser using an electro-optic modulator. Opt Commun 218:337–344

Mercier D, Pothier A, Blondy P (2003) Monitoring mechanical characteristics of MEMS switches with a microwave test bench, 4th Round Table on Micro and Nano technologies for Space, Noordwijk, Netherlands

Muldavin J, Boisvert R, Bozler C, Rabe S, Keast C (2003) Power handling and linearity of MEM capacitive series switches. Microwave Symposium Digest, IEEE MTT-S International 3:1915–1918

Russo NA, Duchowicz R, Mora J, Cruz JL, Andrés MV (2002) High-efficiency Q-switched erbium fiber laser using a Bragg grating-based modulator. Opt Commun 210:361–366

Zalvidea DD, Russo NA, Duchowicz R, Delgado-Pinar M, Dýez A, Cruz JL, Andrés MV (2005) High-repetition rate acoustic-induced Q-switched all-fiber laser. Opt Commun 244:315–319

Zhu Y, Espinosa HD (2004) Effect of temperature on capacitive RF MEMS switch performance-a coupled-field analysis. J Micro Mech Micro Eng 14:1270–1279